

Hexagonal convection cells under conditions of vertical symmetry

R. M. Clever and F. H. Busse

*Institute of Geophysics and Planetary Physics, University of California at Los Angeles, Los Angeles, California 90024
and Institute of Physics, University of Bayreuth, D-95440 Bayreuth, Germany*

(Received 28 November 1995)

The stability of hexagonal convection cells is analyzed in the case of a Boussinesq fluid heated from below with symmetric rigid horizontal boundaries. For $P > 1.2$ a region of stable hexagon convection appears for $\alpha < \alpha_c$ and $R \geq 2R_c$ where P , α , R are the Prandtl number, the wave number, and the Rayleigh number. The theoretical results are in agreement with recent experimental observations by Assenheimer and Steinberg [Phys. Rev. Lett. **76**, 756 (1996)].

PACS number(s): 47.20.Ky, 47.27.-i

I. INTRODUCTION

Hexagonal cells are a well known manifestation of convection flows in fluid layers heated from below. They are often called Bénard cells after the scientist who first conducted extensive experiments on thermal convection [1]. Later experimental studies [2,3] have demonstrated that hexagonal convection cells compete with roll-like convection. In agreement with the theoretical predictions (see, for example, [4]) it was shown that the range of stable hexagonal cells tends to zero as the asymmetry of material properties about the midplane of the fluid layer vanishes. The original experiments of Bénard were carried out under strongly asymmetric conditions in that the temperature dependence of the surface tension provided the main driving force for the convection flow [5,6]. The preference for hexagons owing to asymmetries becomes clear when it is remembered that there are two types of hexagonal cells differing by the direction of motion in the center. Rising motion in the center of the cells is typically found in liquids which are characterized by decreasing viscosity with increasing temperature in contrast to gases for which viscosity tends to increase with temperature. Convection in gases does indeed exhibit descending flow in the cell center [7] since that direction of motion is preferred for which the region of highest rate of strain, namely the center, corresponds to the lowest viscosity of the convection cell. Accordingly only one of two types of hexagonal cells is expected to be realized in any experiment.

In view of the well understood competition between rolls and hexagons near the onset of convection, the recent observations by Assenheimer and Steinberg [8] of both types of hexagonal cells at the same time in a convection layer with only minimal asymmetric properties are highly surprising. It is important to note that the Rayleigh number R was not close to the critical value R_c for onset of convection, which indicates that a theoretical description of the phenomenon cannot be derived from a weakly nonlinear analysis. In this paper we describe computations which indicate that hexagonal convection cells of both types become stable at Rayleigh numbers of about two times the critical value if the Prandtl number P exceeds a value of the order unity.

In the following we briefly outline the mathematical problem and the numerical method used for its solution. The main task is the analysis of the stability of steady hexagon

solutions with respect to infinitesimal disturbances. There are not yet sufficient experimental data available for detailed comparisons with the theory. But the observations reported so far are in agreement with the theoretical predictions.

II. MATHEMATICAL FORMULATION OF THE PROBLEM

We consider a horizontal fluid layer of depth h with the temperatures T_1 and T_2 prescribed at the upper and lower rigid boundaries. Using h as length scale, h^2/κ as time scale where κ is the thermal diffusivity of the fluid, and $T_2 - T_1$ as temperature scale we can write the equations of motion for the velocity vector \vec{u} and the heat equation for the deviation θ of the temperature field from the static solution of the problem in the nondimensional form

$$P^{-1} \left(\frac{\partial \vec{u}}{\partial t} + \vec{u} \cdot \vec{\nabla} \vec{u} \right) = -\vec{\nabla} \pi + \vec{\lambda} \theta R + \nabla^2 \vec{u}, \quad (1a)$$

$$\vec{\nabla} \cdot \vec{u} = 0, \quad (1b)$$

$$\frac{\partial \theta}{\partial t} + \vec{u} \cdot \vec{\nabla} \theta = \vec{\lambda} \cdot \vec{u} + \nabla^2 \theta, \quad (1c)$$

where $\vec{\lambda}$ is the unit vector in the vertical direction, π is the deviation of the pressure from its static value, and where the Rayleigh number R and the Prandtl number P are defined by

$$R = \frac{\gamma(T_2 - T_1)gh^3}{\nu\kappa}, \quad P = \frac{\nu}{\kappa}. \quad (2)$$

Here g , γ , and ν denote the acceleration of gravity, the thermal expansivity, and kinematic viscosity, respectively. It is convenient to eliminate Eq. (1b) through the introduction of the general representation for solenoidal vector fields

$$\vec{u} = \vec{\nabla} \times (\vec{\nabla} \times \vec{\lambda} \varphi) + \vec{\nabla} \times \vec{\lambda} \psi. \quad (3)$$

Steady three-dimensional solutions of Eqs. (1) can be obtained through the Galerkin ansatz

$$\varphi = \sum_{l,m,n} \{ \cos l x (a_{l m n}^{c c} \cos m y + a_{l m n}^{c s} \sin m y) + \sin l x (a_{l m n}^{s c} \cos m y + a_{l m n}^{s s} \sin m y) \} f_n(z), \quad (4a)$$

$$\theta = \sum_{l,m,n} \{ \cos l x (b_{l m n}^{c c} \cos m y + b_{l m n}^{c s} \sin m y) + \sin l x (b_{l m n}^{s c} \cos m y + b_{l m n}^{s s} \sin m y) \} \sin \pi (z + \frac{1}{2}), \quad (4b)$$

$$\psi = \sum_{l,m,n} \{ \sin l x (c_{l m n}^{c c} \sin m y + c_{l m n}^{c s} \cos m y) + \cos l x (c_{l m n}^{s c} \sin m y + c_{l m n}^{s s} \cos m y) \} \sin \pi (z + \frac{1}{2}), \quad (4c)$$

where we have introduced a Cartesian system of coordinates with the z coordinate in the vertical direction and where $f_n(z)$ denotes the Chandrasekhar functions [9] which have the property $f_n = df_n/dz = 0$ at $z = \pm \frac{1}{2}$. In this way representation (4) ensures that the conditions at the rigid boundaries

$$\varphi = \partial \varphi / \partial z = \theta = \psi = 0 \quad \text{at } z = \pm \frac{1}{2} \quad (5)$$

$$a_{l m n}^{i j} = b_{l m n}^{i j} = c_{l m n}^{i j} = 0 \quad \text{for } l+m = \text{odd (a) and also for } l+m = \text{even, unless } i=j=c \text{ (b)}. \quad (7)$$

An example of solutions of this kind is shown in Fig. 1. The wave number of hexagon solutions is traditionally described by $\alpha = 2b$ since the coefficients $a_{111}^{c c}, a_{201}^{c c}$ become the dominant ones as the critical value of the Rayleigh number, $R_c = 1708$ with $\alpha_c = 3.116$, is approached. In Fig. 2 the heat transport by hexagonal convection is plotted in comparison with the heat transport by two-dimensional rolls. The Nusselt number Nu is defined as the total heat transport divided by the heat transport in the absence of convection. As is evident from the figure, Nu depends more strongly on the basic wave number of convection than on the Prandtl number, at least in the regime $P \geq 1$. In contrast to the situation at Rayleigh numbers right above the critical value where the heat transport by convection rolls exceeds that of hexagonal convection [10], the latter type of convection becomes more efficient than the former in transporting heat as the Rayleigh number is increased. This effect may be caused in part by the higher harmonics in the horizontal dependence which are stronger for the hexagon solution than for two-dimensional convection.

IV. STABILITY ANALYSIS OF STEADY HEXAGONS

The stability of steady hexagon solutions characterized by the parameters R, P , and α can be investigated through the imposition of arbitrary infinitesimal disturbances $\tilde{\varphi}, \tilde{\theta}, \tilde{\psi}$. For these the same representation (4) holds as for the spatially periodic steady solutions except that the factor $\exp\{i dx + i e y + \sigma t\}$ multiplies each expression. In the fol-

lowing we shall restrict the analysis to disturbances with $d=e=0$ which do not change the horizontal periodicity interval of the steady solution, $0 \leq x \leq 4\pi/\sqrt{3}\alpha$, $0 \leq y \leq 4\pi/\alpha$. As is evident from Fig. 1, this interval corresponds to the area of two hexagonal cells and the restriction of the periodicity interval is thus not a severe one. In the case $d=e=0$ the stability analysis is much simplified since the disturbances separate into eight classes each of which corresponds to vanishing coefficients $\tilde{a}_{l m n}^{i j}$ except for a single superscript combination i, j and each is characterized by the validity of the symmetry (7a), denoted in the following by E , or by the opposite symmetry, denoted by O . The eight classes are thus described by

$$l+m+n > N_T \quad (6)$$

is satisfied. The truncation parameter N_T is chosen in such a way that global properties, such as the heat transport, are not changed by more than about 1% when N_T is replaced by $N_T - 2$.

III. STEADY HEXAGON SOLUTIONS

Solutions of the form (4) describing hexagonal convection can be obtained when $a = \sqrt{3}b$ is chosen. All coefficients with $l+m = \text{odd}$ vanish for the hexagon solution. Moreover, by replacing the center of the hexagonal cell at $x=y=0$ and using its symmetry we find that the solution can be represented by coefficients with the properties

lowing we shall restrict the analysis to disturbances with $d=e=0$ which do not change the horizontal periodicity interval of the steady solution, $0 \leq x \leq 4\pi/\sqrt{3}\alpha$, $0 \leq y \leq 4\pi/\alpha$. As is evident from Fig. 1, this interval corresponds to the area of two hexagonal cells and the restriction of the periodicity interval is thus not a severe one. In the case $d=e=0$ the stability analysis is much simplified since the disturbances separate into eight classes each of which corresponds to vanishing coefficients $\tilde{a}_{l m n}^{i j}$ except for a single superscript combination i, j and each is characterized by the validity of the symmetry (7a), denoted in the following by E , or by the opposite symmetry, denoted by O . The eight classes are thus described by

$$CCE, CSE, SCE, SSE, CCO, CSO, SCO, SSO. \quad (8)$$

According to this classification the steady hexagon solution belongs to the class CCE . Disturbances that tend to shift the hexagon solution in the x or y direction belong to the classes SCE or CSE , respectively. The linear equations for the unknown coefficients $\tilde{a}_{l m n}, \tilde{b}_{l m n}, \tilde{c}_{l m n}$ for a given hexagon solution give rise to an eigenvalue problem with the growth rate σ as eigenvalue. Whenever there exists an eigenvalue σ among the eight classes (8) with positive real part the hexagon solution is regarded as unstable; otherwise it is regarded as stable, at least with respect to the disturbances which fit the periodicity interval.

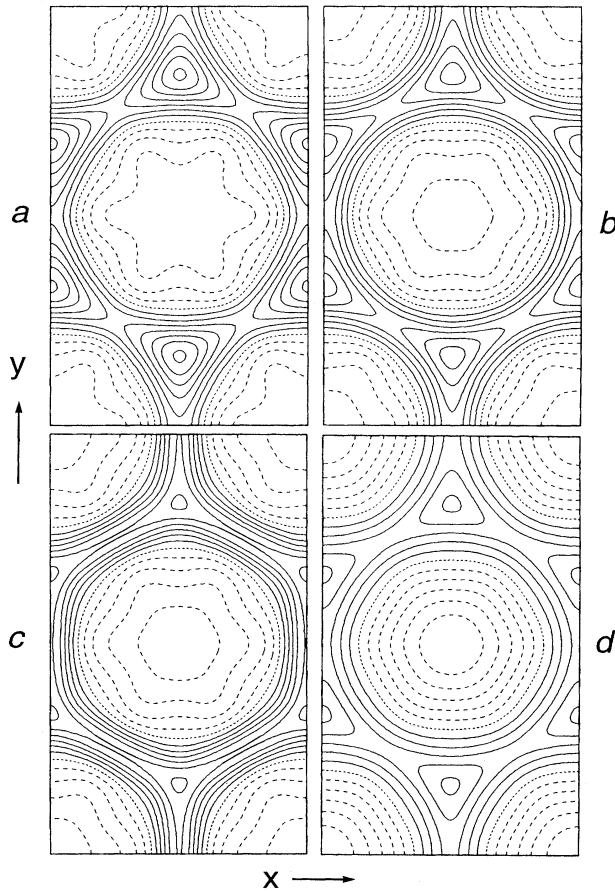


FIG. 1. Lines of constant vertical velocity with solid (dashed) lines for positive (negative) values in the planes $z = -0.4$ (a), $z = 0.4$ (b), $z = 0$ (c), and isotherms in the plane $z = 0$ (d) for hexagonal convection with $R = 5000$, $P = 4.0$, $\alpha = 2.0$. The dotted curves indicate zero.

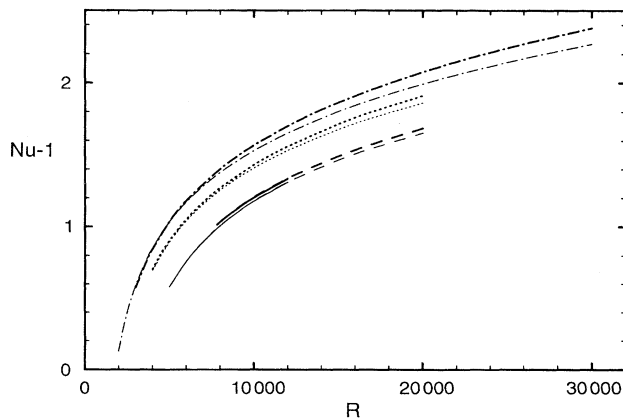


FIG. 2. Nusselt number as a function of R for two-dimensional convection (thin lines) and for hexagonal convection (thick lines) in the cases $P = 2.5$, $\alpha = 1.5$ (solid lines), $P = 4.0$, $\alpha = 1.5$ (dashed lines), $P = 7.0$, $\alpha = 2.0$ (dotted lines), and $P = 16$, $\alpha = 2.5$ (dash-dotted lines).

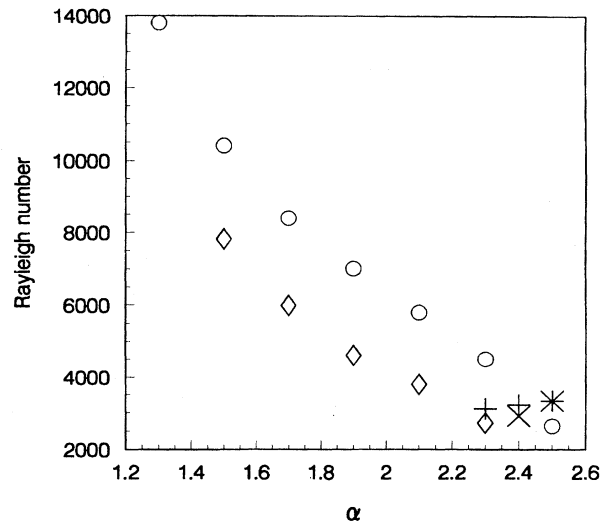


FIG. 3. The region of stable hexagons in the R - α plane for $P = 2.5$ is bounded by the onset of *SCO* disturbances (\circ) from above and *CCO* disturbances (\diamond) from below. At low Rayleigh numbers the stability region is bounded from below by the onset of *SSE* disturbances ($+$) and *CCE* disturbances (\times).

Figures 3–5 show the regions in the R - α plane of stable hexagonal convection for $P = 2.5$, 7, and 16. Stable hexagons always have wave numbers much lower than the critical value α_c . The extent of the stability region towards low wave numbers α could not be determined usually because either steady hexagon solutions with very low wave numbers did not converge or the numerical scheme produced solutions with higher wave numbers. For all Prandtl numbers less than about 10 the region of stable hexagons corresponds to a strip in the R - α plane the average wave number of which decreases with increasing Rayleigh number. No stable hexagons were found for R less than 3000. Growing disturbances of the *CCE* or *SSE* class restrict the stability region at the lowermost end. But the bulk of the stability region is

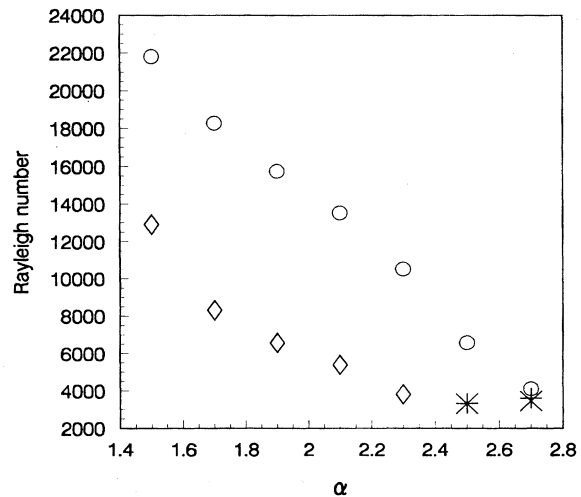


FIG. 4. Same as Fig. 3, but for $P = 7$.

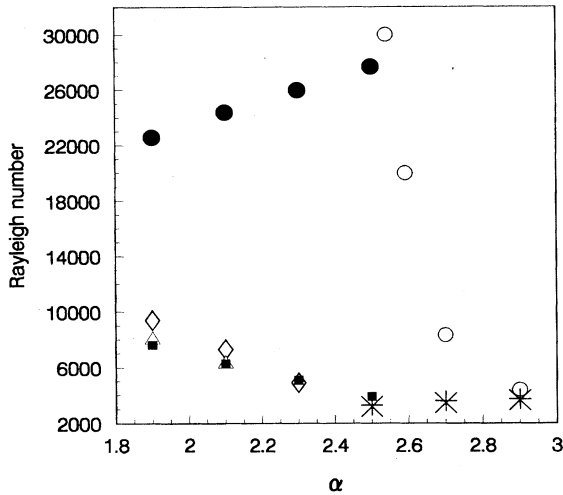


FIG. 5. Same as Fig. 3, but for $P=16$. In addition to the previously mentioned instabilities the region of stable hexagons is also bounded by the onset of CCO disturbances (●) from above, and by the onset of SCO disturbances (Δ), and SSO disturbances (■) from below.

bounded by growing CCO disturbances towards low R and by growing SCO disturbances towards high R . Only in the case $P=16$ more complex stability boundaries are obtained. All instabilities involved in the stability boundaries are characterized by a vanishing imaginary part of the growth rate σ thus indicating monotonic rather than oscillating instabilities. To ensure that the uncertainty of the stability boundaries is less than about 2% of the Rayleigh number, the truncation parameter N_T has been increased to 20 in some cases. The same truncation was employed for the steady solution and its disturbances.

To demonstrate the disappearance of stable hexagons for low Prandtl numbers, maximum growth rates are shown in Fig. 6 as a function of the Rayleigh number for different Prandtl numbers. Especially the growth rate of SCO disturbances, which grows rapidly with decreasing P , is responsible for the disappearance of the region of stable hexagons.

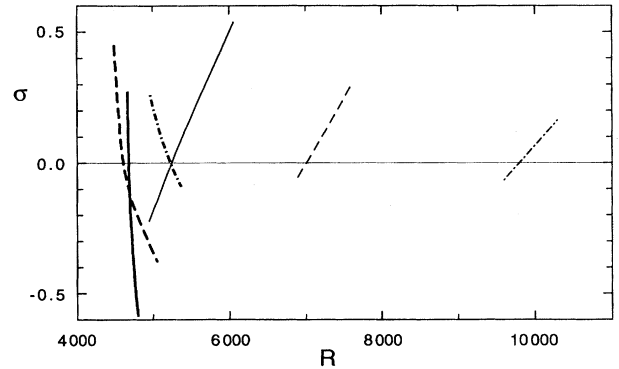


FIG. 6. Growth rates σ of SCO disturbances (thin lines) and CCO disturbances (thick lines) as a function of the Rayleigh number R in the case of steady hexagon solutions with $\alpha=1.9$ for $P=1.5$ (solid lines), 2.5 (dashed lines), and 4.0 (dash-dotted lines).

An extrapolation based on the results presented in Fig. 6 suggests that no stable hexagons will exist for $P \lesssim 1.2$.

V. DISCUSSION

The region of stable hexagons which is identical for both types of hexagon solutions suggests that depending on initial conditions other forms of convection besides convection rolls can be realized in a layer of a Boussinesq fluid heated from below at elevated Rayleigh numbers. This result agrees with the experimental observations of Assenheimer and Steinberg [8]. These authors found coexisting up- and down-hexagons for Prandtl numbers in excess of 2. They also observed that the wavelength is significantly larger than that of rolls in the same experiment. These two features agree well with the theoretical results. Further quantitative agreement is expected once more detailed measurements become available. Of particular interest will be the transition from hexagons to other forms of convection through the evolution of the various instabilities. This will be the subject of future research.

ACKNOWLEDGMENT

The support of the research by the Atmospheric Sciences Section of NSF is gratefully acknowledged.

[1] H. Bénard, *Ann. Chim. Phys./Ser.* **23**, 62 (1901).
 [2] R. W. Walden and G. Ahlers, *J. Fluid Mech.* **109**, 89 (1981).
 [3] P. L. Silveston, *Forsch. Ing. Wes.* **24**, 59 (1958).
 [4] F. H. Busse, *J. Fluid Mech.* **30**, 625 (1967).
 [5] M. J. Block, *Nature (London)* **178**, 650 (1956).
 [6] J. R. A. Pearson, *J. Fluid Mech.* **4**, 489 (1958).
 [7] A. Graham, *Philos. Trans. R. Soc. London Ser. A* **232**, 285

(1933).
 [8] M. Assenheimer and V. Steinberg, *Phys. Rev. Lett.* **76**, 756 (1996).
 [9] S. Chandrasekhar, *Hydrodynamic and Hydromagnetic Stability* (Clarendon Press, Oxford, 1961), pp. 634–636.
 [10] A. Schlüter, D. Lortz, and F. H. Busse, *J. Fluid Mech.* **23**, 129 (1965).